Modelling the Plant Microtubule Cytoskeleton

Eva E. Deinum and Bela M. Mulder

Abstract In this chapter we introduce the plant cortical microtubule array. This structure is both a nexus in the control of plant cell shape and function, and a fascinating out-of-equilibrium system for state-of-the art physics research. We describe how analytical and computational approaches complement each other in the study of the array, and highlight some recent results and open research questions.

1 Microtubules: dynamic controllers of plant cell growth and development

Plant cells distinguish themselves from other eukaryotic cells by being encased in a rigid cell wall. These walls are composed of long cellulose microfibrils embedded in a matrix consisting of a complex mixture of other polysaccharides [1]. The cells typically adopt strongly anisotropic shapes requiring a significant degree of control over the way they grow. Moreover, the typical dimensions of plant cells in the range of 10μm to 100μm exceed those of most mammalian cells. This implies that plant cells require the means to sense and control their geometry on the scale of 10's of μm's. A major molecular workhorse in providing these key services is the microtubule (MT) cytoskeleton. It is composed of long and highly dynamic filamentous protein polymers [2] that, aided-and-abetted by a class of microtubule associated proteins (MAPs) [3], are able to self-organize into a number of cell-scale functional structures. In order of appearance during the cell cycle they are the cortical array (CA), the pre-prophase band, the mitotic spindle and the phragmoplast.

Eva Deinum
Mathematical and Statistical Methods, Wageningen University & Research, the Netherlands e-mail: eva.deinum@wur.nl

Bela Mulder
AMOLF, Amsterdam and Laboratory of Cell Biology, Wageningen University & Research, the Netherlands e-mail: mulder@amolf.nl

Of these four, the CA [4], the pre-prophase band [5] and the phragmoplast [6] are plant specific. Even the plant mitotic spindle, although overall similar in shape to its mammalian counterpart, does have significant structural differences to the latter [7]. MTs in mammalian cells are associated to so-called centrosomes [8], which act as hubs for their nucleation and typically dictate a radial organisation. Plant cells do not have centrosomes, which implies that other organisational principles must be at play [9]. Of the four MT structures mentioned above, the CA has to date received the most interest. The CA invariably appears in growing plant cells and is composed of MTs roughly homogeneously dispersed over the entire cell cortex, which are oriented in a direction transverse to the growth axis of the cell.

2 Dynamic self-organisation: exciting biology and challenging physics/mathematics

What makes structures like the CA doubly interesting is that they are apparently self-organising [10]. In root epidermal cells, the CA develops in approximately one hour after cytokinesis from an initial state in which the cortex which is devoid of any MTs. More strikingly, while a fully developed CA can be totally disrupted by adding MT-depolymerizing drugs such as oryzalin, it returns to its original state within an hour after these drugs are washed out. This obviously speaks for their robustness from the point of view of biological functionality. At the same this means that the CA poses the challenging question of which mechanism(s) drive and control its formation. The CA is composed of 1000's of MTs, each of which is a stochastic dynamical system in its own right. Somehow, through interactions between these dynamical actors a state is reached which has well-defined and stable global properties, in spite of the unceasing stochastic activity of its elements. From the point of view of statistical physics, this characterizes the CA as a far out of equilibrium steady state of an ensemble of interacting spatially extended particles. Such systems represent the cutting edge of our physical understanding [11].

3 MT behaviour at different levels of description

3.1 At the MT level: dynamic instability

Individual MTs are highly dynamic protein structures. They are long (up to many μm), thin (about 25 nm in diameter) and polar. Growth and shrinkage of MTs occurs at their ends, which are called "plus" and "minus". MT behaviour can be described at many different levels, with consequences for the kinds of questions that can be tackled with a certain description. The basic building blocks of MTs are α,β-tubulin heterodimers. These subunits form chains, and typically 13 of these

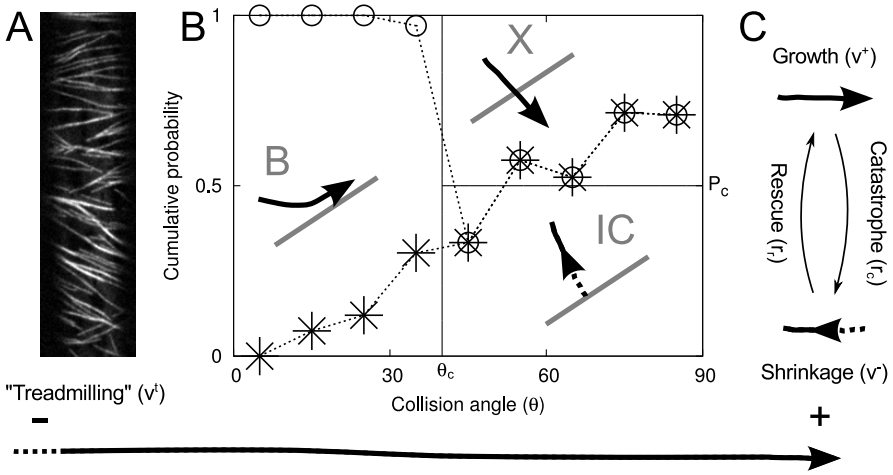

Fig. 1 A: Cortical array in an *A. thaliana* hypocotyl cell(confocal microscope image courtesy J.J. Lindeboom, Stanford). B: Interaction between MTs. Depending on the relative angle θ, a collision may result in bundling (grey B), or an induced catastrophe (grey IC, with probability P_c) or crossover (grey X). C: Dynamic instability at the MT plus end.

so-called protofilaments together form an MT. The plus end of the MT is highly dynamic: it may grow through polymerization, the incorporation of new subunits, shrink through depolymerization or pause. Switches between growth and shrinkage are called catastrophes and rescues. The minus end is also dynamic, but with different kinetic parameters, and typically has a tendency towards net depolymerization.

If you are interested in understanding or predicting the parameters that describe this so-called dynamic instability, you have to consider many molecular details. Tubulin subunits are incorporated in a GTP-bound state, and stochastically get hydrolized into a GDP-state. Protofilaments of GTP-tubulin are almost straight, but GDP-tubulin protofilaments have a tendency to curve. Consequently, a growing MT is stabilized by a "straight" cap of GTP-tubulin. If this cap disappears, however, due to depletion of free subunits, delayed growth caused by some obstruction, or whatever other reason, the protofilaments start curving outward and the plus end starts shrinking fast: a catastrophe. To understand the process of a rescue, one/you more over has/have to consider the many kinds of proteins that interact with MTs. Detailed molecular models may help predict how mutations in tubulin or other relevant proteins affect MT dynamics.

3.2 At the cell level: interactions

Understanding the behaviour of the entire cortical array, on the other hand, is easier with a much simplified model of MT dynamics (figure 1). Disregarding all

molecular detail, growth and shrinkage may be described with one constant (average) velocity each, and the transitions may be described with constant rates. For many questions, we may entirely forget about the pause state and map a 3-state (growth/shrinkage/pause) description onto a 2-state (growth/shrinkage description) [12].

Similarly, nucleation of new MTs occurs mostly from existing MTs and with specific distributions of relative angles between parent and child [13]. These distributions, in turn, can be tuned by the plant. Nucleation complexes, moreover, are about 10 times more active when associated with an MT than when not [14]. Depending on the questions you are interested in, it may be important to incorporate many details of the nucleation process, a caricature of the process that can be described with one or few parameters, or simple isotropic nucleation may even suffice.

And what about the cell itself? Is it sufficient to describe the cell cortex as a simple periodic surface of an appropriate size, is it essential to approximate the shape of real plant cells as close as possible, or would some simple geometry like a box or cylinder be better? That, too, depends on the question.

The MTs comprising the CA are attached to the cell membrane. This essentially reduces the CA to an (almost) two dimensional system. Consequently, growing MTs will frequently collide into other, obstructing, MTs. Modelling studies of the CA were sparked by the observations by Dixit and Cyr [15] that the outcomes of such collisions strongly depend on the relative angle (θ) between incoming and obstructing MT (figure 1). For shallow angle interactions ($\theta \lesssim 40^\circ$), the incoming MT will typically continue growing along the obstructing MT, a process referred to as bundling (or sometimes as zippering or entrainment). For larger angle interactions, the MT may either continue growing in its original direction ("crossover") or, typically after a short pause, start shrinking ("induced catastrophe").

The observation of these angle dependent collision outcomes immediately raised the question: are these interactions, combined with the standard MT dynamic instability, sufficient for spontaneous self-organization of the CA? Several groups approached this question using models, both analytical [16, 17, 18] and computational [19, 20, 21, 12].These approaches complement each other, for example, see section 6.

3.3 At the tissue level: coarse graining

Going up to the tissue level, cell expansion properties must be coordinated to ensure tissue coherence, especially during growth. Such coordination may be achieved through simultaneous responses to the same external cue, for example in blue light induced reorientation of the array [22], with mobile developmental signals such as a plant hormones [23], or in response to tissue spanning stresses [24]. With regard to the latter: a correlation between stresses in the cell wall and the net orientation of the CA is observed in certain cell types [25, 26]. Current models of this phenomenon ignore the mechanistic basis of this correlation and explore its conse-

quences in mechanical models which describe the entire CA with just two numbers per cell [25, 27, 28].

4 The consensus model of MT dynamics

Following the discussion above, we focus on what has become the generally accepted model for describing MT dynamics in the CA. In this model MTs live and die in a 2-dimensional domain which represents (part of the) the cell cortex. They are born through nucleation events that can occur either at random locations within this domain, in which case their initial growth direction is also random, or from a random position on the body of an existing MT, in which case their initial orientation may depend on that of the parent MT. MTs are taken to be composed of straight line segments, where on curved surfaces "straight" translates into a following a geodesic path. The plus-end tip of growing MT moves with the growth speed v^+, while if applicable the minus-end retracts with the treadmilling speed v^t. A growing MT can switch to the shrinking state with the constant catastrophe rate r_c. The plus-end of a shrinking MT retracts with a speed v^- and can switch to the growing with the rescue rate r_r. When the tip of a growing MT collides with another MT, the outcome depends on the angle of incidence θ. Whenever this angle is below the critical angle $\theta_c = 40^o$, a bundling event occurs. At a bundling event a new segment of the colliding MT is created, along the obstructing MT. In this way, an MT can consist of multiple segments, each with its own orientation and length. Only the front segment is *active* and either in the growing or the shrinking state. The remaining segments are *inactive*, except in the case of minus-end retraction in which the rear segment is always shrinking. Inactive segments can thus be *reactivated* when they start shrinking either at their plus- or their minus-end. When at a collision the incidence angle is above θ_c, the MT undergoes an induced catastrophe with probability $0 < P_c < 1$, where $P_c = 0.5$ is often chosen as default. Finally, when an MT shrinks to length 0 it simply disappears.

5 Simulations: Time steps versus event driven

As described above, simulation studies addressing the question of array alignment model individual MTs as connected sets of line segments that switch between growth, shrinkage and possibly pausing at the plus end, and have either stable or steadily retracting minus ends. There are essentially two ways of implementing these phenomena in a simulation: using discrete time steps or with an event driven algorithm.

With *discrete time steps*, all plus (and minus) ends are updated every time step (Δt). Simple cases are when they grow a certain length ($v^+\Delta t$) without obstruction, or shrink ($v^-\Delta t$) during the whole time step: the tip's is propagated by the specified

length and that's it. Additionally, tips may switch state during the time step with certain probability (r_c, r_r, ...). This may sound simple enough, but you have to think carefully about the length change of the MT during this time step: depending on when during the time step it presumptively has switched, it may show net growth, shrinkage, or no change of length. The difference between (the extremes of) these options, of course, decrease with shorter time steps, but that has a computational cost.

When the length increase of a growing MT brings it across an obstructing MT, the resulting interaction must be handled: for example, if this resulted in a bundling event, the new position of the plus tip will be along the obstructing MT, at a distance beyond the intersection the length of its initial overshoot.

Handling these interactions one by one works as long as it is safe to assume that they are all independent. With increasing Δt, however, the probability increases that MT changes become interdependent. For example, an early updated plus end may undergo bundling onto an MT that itself undergoes a (spontaneous or induced) catastrophe in the same time step – effectively resulting in bundling onto empty space. As you can see, this method requires a lot of careful thinking and bookkeeping that is not apparent from the simple idea behind the algorithm. The problem of interdependent interactions/state changes not only aggravates with longer time steps, but also with increasing array density. Consequently, the maximum allowable time step size may turn out to be so small, that it becomes hard to obtain good simulation statistics of large or high density arrays.

In *event driven* simulations, the problems of event interdependence and the uncertainty of MT length after a state switch are solved. The essence of event driven simulations is that events (interactions among MTs, spontaneous state changes, and even measurements) are scheduled against a continuous wall clock. These events are handled one by one and, where necessary, the probabilities of particular event types are adjusted after each event. Calculating future event times requires forward integrating the equations of tip motion (for growth and shrinkage, which are *deterministic events*), or drawing random numbers based on the probability density of *stochastic events*.

If done in a smart way, such event-driven simulations can be very computationally efficient. We review some concepts that help keep the simulations efficient [12, 29]. First of all, as MT are modelled using straight line segments, it is possible to compute exactly when a growing MT may interact with another one by extrapolating MT paths. The intersections between such lines ("trajectories" in [12]) can be precomputed and will be the same for all MTs within a bundle. To keep the computational cost of computing trajectory intersections sufficiently low, the simulation domain may be subdivided into smaller parts.

For stochastic events (rescues, spontaneous catastrophes, MT nucleation, ...), we only need to know the event time of the first event. If the first stochastic event is scheduled before the first deterministic event, it is executed, and the first deterministic event otherwise. In the former case, the type of stochastic event and its specifics are selected proportional to the respective rates.

In general, the time interval Δt_s until the next stochastic event can be calculated from

$$\int_t^{t+\Delta t_s} R(\tau)\mathrm{d}\tau = -\log u \tag{1}$$

with $R(t)$ the sum of all instantaneous rates $r_i(t)$ for all different stochastic event types and u a uniform random variate on the interval (0,1). If all event types have constant rates *between two events*, then

$$R(t) = R = \sum_i r_i \tag{2}$$

and

$$\Delta t_s = -\frac{\log u}{R}. \tag{3}$$

For examples of non-constant rates we refer to [12].

After an event, it is likely that the rates of some event types have changed slightly, for example, because the number of growing MTs has changed. This shows that it is not only not necessary to calculate more than one stochastic event ahead, but also wrong: the times of many later events would have been drawn according to outdated waiting time distributions.

Scheduling events with a constant rate is easy, as their waiting times all follow exponential distributions. Some rates, however, may not be constant over time. In that case there are two major options. The first is to calculate the correct waiting time distribution of the variable rate and sample according to that. The second is to use a rejection method: schedule events with a constant rate corresponding to the highest possible instantaneous rate and if the event is selected for execution, only execute it with probability instantaneous rate / maximum rate. The validity of the latter option depends on the Markov property of the model: the behaviour of the system is fully determined by its current state. Which of these two options is best depends on how hard it is to compute the exact waiting time distribution –mathematically but also computationally– and the difference between maximum rate and average instantaneous rate.

Finally, considerable computational savings are possible by only updating the necessary information. The positions of all MT ends must be known exactly for measuring the state of the array, but not for the correct scheduling and execution of events. The number of growing and shrinking MTs is enough to calculate, for example, how the total MT length and density change between events, which in turn is sufficient to correctly schedule all events that depend on these quantities.

6 Understanding order

Before discussing how order comes about, we first need to define a *quantitative measure* of the degree of order. To that end we employ the notion of an *order parameter*. Order parameters have a long history in physics [30], and are widely used

to distinguish different macroscopic states of physical systems. The one appropriate to describe the orientational order of line-like objects independent of their polarity, is

$$S_2 = \sqrt{\langle \cos(2\theta) \rangle^2 + \langle \sin(2\theta) \rangle^2} \tag{4}$$

where θ is the angle of the MT segments with respect to an arbitrary, but fixed, axis in the plane, and the angle brackets $\langle \cdots \rangle$ denote taking the length weighted average over many microstates in the steady state. If the all directions are equally abundant, we find $\langle \cos(2\theta) \rangle = \langle \sin(2\theta) \rangle = 0$ and hence $S_2 = 0$, which characterizes the disordered state. On the other hand, if all segments have exactly the same orientation θ_0, then $S_2 = \sqrt{\cos^2(2\theta_0) + \sin^2(2\theta_0)} = 1$, which marks the fully ordered state. In this way S_2 creates a natural scale measuring the degree of order between the limits 0 and 1.

In order to understand how ordering could in principle arise in a system of dynamical MTs interacting in the manner described in section 4, an analytical approach is indispensable. First of all, such a theory allows one to establish a direct link between the assumptions of the underlying model and the outcomes. Moreover, through a combination of structural and dimensional analysis of the formulated equations the "true" parameters that determine the behaviour of the system are revealed. Finally, the results of theory can be used to provide an independent validation of simulation results. In our analytical approach we forgo the description of individual MTs, but rather focus on probability densities per unit of their properties in a large statistical ensemble of equivalent systems. The basic dependent variables we consider are $m_i^+(l,\theta,t)$, $m_i^-(l,\theta,t)$ and $m_i^0(l,\theta,t)$ being respectively the density of growing, shrinking and dormant segments of length l, orientation θ at time t that are the product of i prior bundling events. The evolution equations for these densities are schematically of the form

$$\frac{\partial}{\partial t} m_i^+(l,\theta,t) = \Phi_{\text{growth}} + \Phi_{\text{rescue}} - \Phi_{\text{cat}} - \Phi_{\text{ind cat}} - \Phi_{\text{bundle}} \tag{5}$$

$$\frac{\partial}{\partial t} m_i^-(l,\theta,t) = \Phi_{\text{shrink}} - \Phi_{\text{rescue}} + \Phi_{\text{cat}} + \Phi_{\text{ind cat}} + \Phi_{\text{reactivate}} \tag{6}$$

$$\frac{\partial}{\partial t} m_i^0(l,\theta,t) = \Phi_{\text{bundle}} - \Phi_{\text{reactivate}} \tag{7}$$

The fluxes on the right denote the effects of the different process that contribute to the changes of the densities, with the sign indicative of whether it is effectively a gain or a loss term. In addition there is a boundary condition that describes the nucleation of new MTs, which in the simplest case of uniform MT-independent nucleation is $v^+ m_0^+(0,\theta,t) = r_n/2\pi$, where r_n is the nucleation rate per unit area. The set of equations (5)-(7) unfortunately is intractable in the general case. However, if we assume that a steady is reached, things simplify enormously. The first observation is that the length dependence of all densities are exponential, with a single orientation dependent length scale

$$m_i^+(l,\theta) = m_i^+(\theta)e^{-l/l(\theta)} \tag{8}$$

$$m_i^-(l,\theta) = \frac{v^-}{v^+} m_i^+(l,\theta) \tag{9}$$

$$m_i^0(l,\theta) = (1+\frac{v^-}{v^+})Q(\theta)m_i^+(l,\theta) \tag{10}$$

The mean length of segments $l(\theta)$ in a given direction depends on the total intensity of collisions that lead to either an induced catastrophe or a bundling event

$$\frac{1}{l(\theta)} = \frac{1}{\bar{l}} + \int d\theta' \sin(|\theta-\theta'|)\{H(\theta_c - |\theta-\theta'|) + P_c H(|\theta-\theta'|-\theta_c)\}k(\theta') \tag{11}$$

Here $k(\theta)$ is the total length density of segments with orientation θ that forms the "target" which growing segments can hit, $\bar{l}$ is the mean length of an MT in the absence of any collisions, and $H(x)$ is the Heaviside step function. Clearly, the more collisions in a certain direction the shorter the filaments in that direction will be come. This reveals the basic mechanism by which an ordered state can maintain itself: an MT segment aligned with the majority will suffer fewer state changing collisions and is therefore likely to be longer than less fortunate segments who are oriented differently from the majority. Without going into the details, there are three more equations needed for the full description, which together fix, next to the average segment length $l(\theta)$ and total segment length density $k(\theta)$ already mentioned, the ratio between active and passive segments $Q(\theta)$, which already appeared in (10), and $t(\theta)$ the density of active tips. While in principle the nature of the steady states depends on all five MT dynamical parameters r_n,v^+,v^-,r_c and r_r, an appropriate choice of the units length shows that only the ratio

$$G = -\frac{l_0}{\bar{l}} = -\left(\frac{2v^+v^-}{r_n(v^+ + v^-)}\right)^{\frac{1}{3}}\left(\frac{r_r}{v^-} - \frac{r_c}{v^+}\right) \tag{12}$$

is important. The perhaps surprising choice of the minus sign ensures that the larger G , the larger the average length of the MTs. In fact, we limit ourselves to the regime $G < 0$, where the MTs are in the bounded growth regime. For $G > 0$ MTs could in principle grow unbounded in length, and a steady state is no longer possible. The utility of the control parameter G extends far beyond the theory itself. As we have also validated by simulation, it predicts that systems that have very different different dynamical parameters will still show the same self-organisation if their G value is the same. The strategy to deal with this still arguably complex set of coupled equations is the following. One can show that the assumption that all four unknowns $l(\theta)$,$k(\theta)$,$Q(\theta)$ and $t(\theta)$ do *not* depend on θ, works for any value G. This yields the so-called isotropic solution to the equations. However, because the equations are non-linear this need not be the only solution. To probe for the existence other non-isotropic solutions, we use an approach called bifurcation theory. In bifurcation theory one perturbs the original isotropic solution with an appropriate small anisotropic component, e.g.

$$l(\theta) = l_0 + \varepsilon l_2 \cos(2\theta) \tag{13}$$

where l_0 is isotropic value of the mean segment length and $\varepsilon << 1$ a small quantity. Note that at the outset we assume that although MTs are polarized structures, the collisions between them do not depend on the relative polarity. We therefore expect that inverting the direction of all MTs, i.e. letting θ go to $\pi - \theta$ should not change the solution, hence the choice of perturbation with period π. The perturbed values of the unknowns are then entered into the equations, which are subsequently expanded in orders of ε. Requiring that the perturbed functions are a solution to first order in ε , leads to a soluble set of *linear* equations in the amplitudes l_2, k_2, Q_2 and t_2. This set of so-called bifurcation equations only has a solution for a specific value of the control parameter, which identifies the bifurcation points G^*. Thus, for all values of $G > G^*$ the isotropic solution is no longer stable, and an isotropic state spontaneously will develop. If we work out G^* for the consensus model we find

$$G^* = \left(\frac{2}{\pi} 2P_c \sin(2\theta_c)\right)^{1/3} \left(\frac{\pi - \theta_c}{\sin(2\theta_c)} - 1\right) \tag{14}$$

The most surprising aspect of this result is that if the probability of induced catastrophes vanishes ($P_c = 0$), the critical control parameter goes to the effectively unattainable value $G^* = 0$, implying that you need either infinitely long MTs or infinitely many ($r_n \to \infty$) to achieve ordering. It also implies that bundling by itself cannot be responsible for the ordering process. Thus the induced catastrophes are the driver of the ordering process. How can this be understood? The answer is what we have dubbed the "survival of the aligned" principle. When MTs are (almost) aligned they have few collisions among themselves, and if they do these are likely to lead to bundling rather than induced catastrophes. These aligned MTs will therefore be likely to live for their full lifetime. On the other hand, an MT segment that encounters a set of aligned MTs will suffer many collisions. If at these collisions it has a finite probability of suffering an induced catastrophe, it will likely be switched into the shrinking state. A shrinking MT has a significantly shorter expected lifetime than a growing MT. Hence a discordant MT will likely disappear more quickly from the system than the aligned ones, leaving the latter as the stable majority. Likewise a MT nucleated in the majority direction survives longer than one that is nucleated in another direction, hence the name of the principle.

Armed with these results, we can show the generic behavior our theory of CA ordering predicted as a function of the control parameter G, and how this compares to the results of simulations described in Section 5 (Figure 2).

7 Understanding orientation

The orientation of the CA changes in response to environmental signals [22] as well as internal cues, such as mechanical stresses [25]. How this orientation is controlled

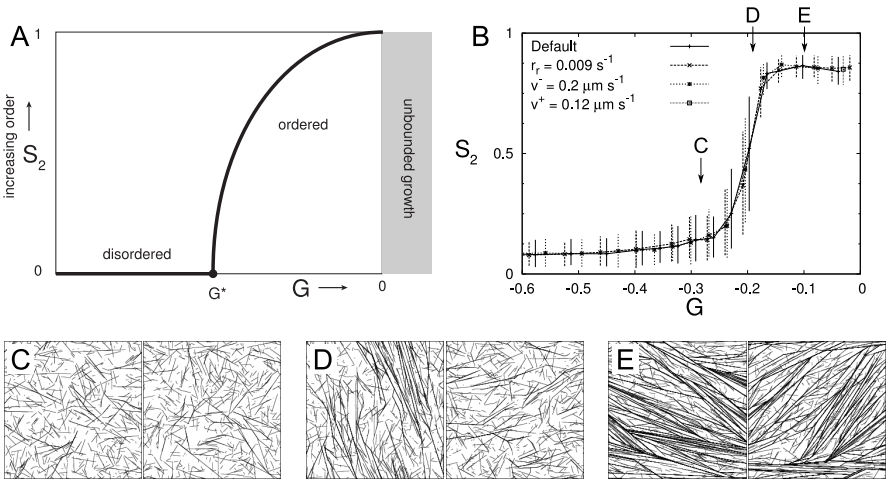

Fig. 2 Understanding order in the CA. A: Theoretically predicted bifurcation diagram. Order arises if $G > G^*$. B: Simulation results: the same G-value can be reached in many different ways. The transition between order and disorder always occurs around the same G-value. C-E: representative snapshots of two simulated CAs per parameter combination as indicated with arrows in B (along the curve with "Default" parameters).

is still an open area of research. In fact, two different processes play a role: first the *de novo* establishment of the array and the concurrent "first" choice of orientation, and second the reorientation of the array.

As stated, the CA is newly established after cell division and also after washout of MT depolymerizing drugs. During both processes a transient population of obliquely oriented MTs is observed, which disappears when the CA adopts is final transverse orientation [29]. The functional importance of this population remains unclear. The current hypothesis is that the oblique MTs disappear because the cell favours only certain orientations. It has been suggested that the sharp corners between cell faces –particularly those to the cell face that was formed during the last cell division– are hard to cross for growing MTs, and that this crossing may be facilitated by the protein CLASP [31]. This suggests a mechanism in which the cell selects a particular orientation through selective facilitation of edge crossing (fig. 3). Even without (controllable) edge crossing penalties, the geometry of the cell itself typically allows only a few orientations [32].

The different orientations allowed by the cell geometry could be seen as local minima in a potential energy landscape. On simple geometries such as rectangular boxes and cylinders, these potential wells correspond to closed paths on the geometry surface that minimize curvature along the path because MTs are stiff. In this interpretation, the establishment of the initial orientation is like finding one of the potential wells and if the difference between different wells is large, most cells are expected to find the global minimum (deepest well). To change orientation, then, would require that the CA is actively "pushed out" of its current well. Making an-

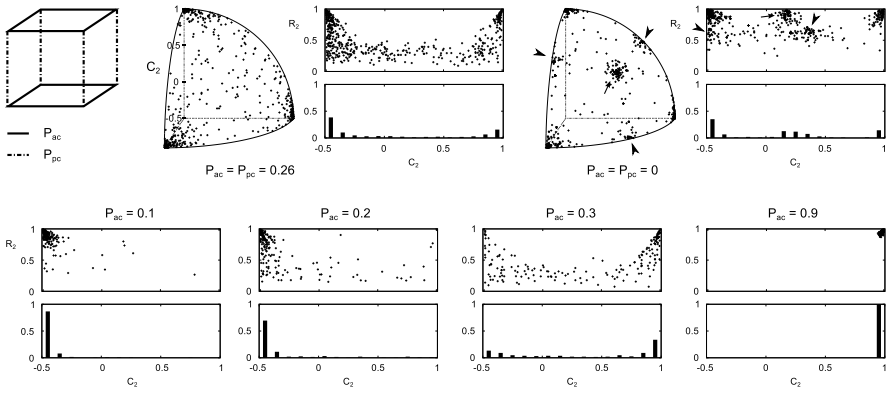

Fig. 3 Cell geometry favours certain orientations. The oblique orientations (arrows and arrow heads) only appear when the penalties for crossing edges (induced catastrophe probabilities P_{ac} and P_{pc}) are 0 or very low. Differences between P_{ac} and P_{pc} may help select between transverse ($C_2 = 1$) and longitudinal ($C_2 = -0.5$) orientations. Cubes are 15x15x15 μm. n=500 simulations per parameter combination. Simulated time T=40000 s. R_2: order parameter between 0 (isotropic) and 1 (perfectly aligned) [12].

other state more favourable (deeper well) alone would be insufficient for reorienting the array. Such active reorientation has indeed been observed in hypocotyl cells that change from transverse to longitudinal CA orientation in response to blue light [22]. During the initial stages of this reorientation process, severing of discordant (oblique and longitudinal) MTs followed by immediate rescues quickly amplifies the population of longitudinal MTs [22].

8 The role of severing

Various experiments have indicated the MT severing enzyme katanin as a key player in inducing alignment in the CA as well as enabling rapid reorientation of the CA in response to environmental signals and cell wall stresses [25, 22] At first sight, this poses a theoretical problem: by the "survival of the aligned" principle, alignment critically depends on having sufficient interactions per MT life time to effectively "weed out" discordant MTs. Random severing along the MT lattice –with new MT plus ends starting in the shrinking state– results in shorter MTs, and hence fewer interactions per MT life time and less alignment [18]. Severing, however, preferentially occurs at MT crossovers and predominantly affects the crossing MT [22, 33]. As the crossing MT is more likely to be a discordant one, this makes crossover severing a delayed punishment of such MTs, effectively contributing to alignment like a weaker form of induced catastrophes [34]. Notably, severing at crossovers only contributes to alignment if shallow angle interactions are protected from severing. Bundling normally offers this protection, because it prevents the formation of

crossovers with small relative angles. This for the first time indicates that bundling *is* important for alignment *in planta* [34]. Understanding how severing can boost alignment also gives a foundation for understanding how severing is important for changes in orientation. Reorientation requires the breakdown of MTs following the old orientation as well amplification of MTs following the new orientation. The latter can be achieved if part of the novel plus ends start in the growing rather than the shrinking state, turning a suppression of the deviant orientation into an amplification [22].

9 Outlook

The CA is a very important structure that bridges developmental signaling and the mechanical execution of growth responses in plants. Modelling studies have played a key role in understanding how the CA self-organizes and will continue to play an important role in understanding CA behaviour. The relative simplicity of the system allows for a high degree of similarity between models and experimental observations, making it possible to quantitatively assess the impact of experimental findings. Currently pressing issues about CA behaviour include its reorientation in response to various internal and external cues. There might be different mechanisms at play in the different reorientation processes, although it seems that katanin often plays a key role [22, 28]. Here, progress in modelling will strongly depend on additional mechanistic insights from cellular observations.

In addition, CA modelling studies so far have focused on homogeneous arrays. For several critical functions and cell types, the array must form inhomogeneous patterns. Striking examples are the condensation of the array into the pre-prophase band prior to cell division [], and the range of patterns found in xylem –where complex CA patterns translate to structured cell walls along a trade-off between element extensibility and resistance against vessel collapse [35].

References

1. D.J. Cosgrove, Nature Reviews Molecular Cell Biology **6**(11), 850 (2005). DOI 10.1038/nrm1746. URL http://www.nature.com/doifinder/10.1038/nrm1746
2. A. Desai, T.J. Mitchison, Annual Review of Cell and Developmental Biology **13**(1), 83 (1997). DOI 10.1146/annurev.cellbio.13.1.83. URL http://www.annualreviews.org/doi/10.1146/annurev.cellbio.13.1.83
3. E. Mandelkow, E.M. Mandelkow, Current Opinion in Cell Biology **7**(1), 72 (1995). DOI 10.1016/0955-0674(95)80047-6. URL http://linkinghub.elsevier.com/retrieve/pii/0955067495800476
4. D.W. Ehrhardt, S.L. Shaw, Annual Review of Plant Biology **57**(1), 859 (2006). DOI 10.1146/annurev.arplant.57.032905.105329. URL http://www.annualreviews.org/doi/10.1146/annurev.arplant.57.032905.105329

5. Y. Mineyuki, (1999), pp. 1–49. DOI 10.1016/S0074-7696(08)62415-8. URL http://linkinghub.elsevier.com/retrieve/pii/S0074769608624158
6. L.G. Smith, Nature Reviews Molecular Cell Biology **2**(1), 33 (2001). DOI 10.1038/35048050. URL http://www.nature.com/doifinder/10.1038/35048050
7. H. Zhang, R.K. Dawe, Chromosome Research **19**(3), 335 (2011). DOI 10.1007/s10577-011-9190-y. URL http://link.springer.com/10.1007/s10577-011-9190-y
8. M. Bornens, Current Opinion in Cell Biology **14**(1), 25 (2002). DOI 10.1016/S0955-0674(01)00290-3. URL http://www.sciencedirect.com/science/article/pii/S0955067401002903
9. D.W. Ehrhardt, Current Opinion in Cell Biology **20**(1), 107 (2008). DOI 10.1016/j.ceb.2007.12.004. URL http://www.sciencedirect.com/science/article/pii/S0955067407001937
10. V.V. Isaeva, Biology Bulletin **39**(2), 110 (2012). DOI 10.1134/S1062359012020069. URL http://link.springer.com/10.1134/S1062359012020069
11. B.A. Grzybowski, C.E. Wilmer, J. Kim, K.P. Browne, K.J.M. Bishop, Soft Matter **5**(6), 1110 (2009). DOI 10.1039/b819321p. URL http://xlink.rsc.org/?DOI=b819321p
12. S.H. Tindemans, E.E. Deinum, J.J. Lindeboom, B. Mulder, Frontiers in Physics **2**(19), 9 (2014). DOI 10.3389/fphy.2014.00019. URL http://www.frontiersin.org/biophysics/10.3389/fphy.2014.00019/abstract
13. J. Chan, A. Sambade, G. Calder, C. Lloyd, Plant Cell **12**(8), 2298 (2009). URL http://eutils.ncbi.nlm.nih.gov/entrez/eutils/elink.fcgi?cmd=prlinks&dbfrom=pubmed&retmode=ref&id=19706794
14. M. Nakamura, D.W. Ehrhardt, T. Hashimoto, Nature Cell Biology **12**(11), 1064 (2010)
15. R. Dixit, R. Cyr, The Plant Cell Online **16**(12), 3274 (2004)
16. S.H. Tindemans, R.J. Hawkins, B.M. Mulder, Phys Rev Lett **104**(5), 058103 (2010). URL http://eutils.ncbi.nlm.nih.gov/entrez/eutils/elink.fcgi?cmd=prlinks&dbfrom=pubmed&retmode=ref&id=20366797
17. R.J. Hawkins, S.H. Tindemans, B.M. Mulder, Physical review. E, Statistical, nonlinear, and soft matter physics **82**(1 Pt 1), 011911 (2010)
18. S.H. Tindemans, B.M. Mulder, Phys Rev E Stat Nonlin Soft Matter Phys **81**(3 Pt 1), 031910 (2010). URL http://eutils.ncbi.nlm.nih.gov/entrez/eutils/elink.fcgi?cmd=prlinks&dbfrom=pubmed&retmode=ref&id=20365773
19. J.F. Allard, G.O. Wasteneys, E.N. Cytrynbaum, Mol Biol Cell **21**(2), 278 (2010). URL http://eutils.ncbi.nlm.nih.gov/entrez/eutils/elink.fcgi?cmd=prlinks&dbfrom=pubmed&retmode=ref&id=19910489
20. E.C. Eren, R. Dixit, N. Gautam, Mol. Biol. Cell **21**(15), 2674 (2010). URL http://eutils.ncbi.nlm.nih.gov/entrez/eutils/elink.fcgi?cmd=prlinks&dbfrom=pubmed&retmode=ref&id=20519434
21. E. Deinum, S. Tindemans, B. Mulder, Phys Biol **8**(5), 056002 (2011). DOI 10.1088/1478-3975/8/5/056002. URL http://dx.doi.org/10.1088/1478-3975/8/5/056002
22. J.J. Lindeboom, M. Nakamura, A. Hibbel, K. Shundyak, R. Gutierrez, T. Ketelaar, A.M.C. Emons, B.M. Mulder, V. Kirik, D.W. Ehrhardt, Science **342**(6163), 1245533 (2013). DOI 10.1126/science.1245533. URL http://dx.doi.org/10.1126/science.1245533
23. L. Vineyard, A. Elliott, S. Dhingra, J.R. Lucas, S.L. Shaw, Plant Cell **25**(2), 662 (2013). DOI 10.1105/tpc.112.107326. URL http://dx.doi.org/10.1105/tpc.112.107326
24. N. Hervieux, M. Dumond, A. Sapala, A.L. Routier-Kierzkowska, D. Kierzkowski, A.H. Roeder, R.S. Smith, A. Boudaoud, O. Hamant, Current Biology **26**(8), 1019 (2016)
25. O. Hamant, M.G. Heisler, H. Jonsson, P. Krupinski, M. Uyttewaal, P. Bokov, F. Corson, P. Sahlin, A. Boudaoud, E.M. Meyerowitz, Y. Couder, J. Traas, Science **322**(5908), 1650 (2008). DOI 10.1126/science.1165594. URL http://www.sciencemag.org/cgi/content/abstract/322/5908/1650

26. M. Uyttewaal, A. Burian, K. Alim, B. Landrein, D. Borowska-Wykrt, A. Dedieu, A. Peaucelle, M. Ludynia, J. Traas, A. Boudaoud, D. Kwiatkowska, O. Hamant, Cell **149**(2), 439 (2012). DOI 10.1016/j.cell.2012.02.048. URL http://dx.doi.org/10.1016/j.cell.2012.02.048
27. M.G. Heisler, O. Hamant, P. Krupinski, M. Uyttewaal, C. Ohno, H. Jönsson, J. Traas, E.M. Meyerowitz, PLoS Biol **8**(10), e1000516 (2010). DOI 10.1371/journal.pbio.1000516. URL http://dx.doi.org/10.1371/journal.pbio.1000516
28. A. Sampathkumar, P. Krupinski, R. Wightman, P. Milani, A. Berquand, A. Boudaoud, O. Hamant, H. Jönsson, E.M. Meyerowitz, Elife **3**, e01967 (2014). DOI 10.7554/eLife.01967. URL http://dx.doi.org/10.7554/eLife.01967
29. J.J. Lindeboom, A. Lioutas, E.E. Deinum, S.H. Tindemans, D.W. Ehrhardt, A.M.C. Emons, J.W. Vos, B.M. Mulder, Plant Physiol **161**(3), 1189 (2013). DOI 10.1104/pp.112.204057. URL http://dx.doi.org/10.1104/pp.112.204057
30. J.P. Sethna, in *1991 Lectures in Complex Systems*, *Santa Fe Institute Studies in Sciences of Complexity*, vol. 15, ed. by L. Nagel, D. Stein (1992), *Santa Fe Institute Studies in Sciences of Complexity*, vol. 15
31. C. Ambrose, J.F. Allard, E.N. Cytrynbaum, G.O. Wasteneys, Nat Commun **2**, 430 (2011). DOI 10.1038/ncomms1444. URL http://dx.doi.org/10.1038/ncomms1444
32. E.E. Deinum, Simple models for complex questions on plant development. Ph.D. thesis (2013)
33. Q. Zhang, E. Fishel, T. Bertroche, R. Dixit, Curr Biol **23**(21), 2191 (2013). DOI 10.1016/j.cub.2013.09.018. URL http://dx.doi.org/10.1016/j.cub.2013.09.018
34. E.E. Deinum, S.H. Tindemans, J.J. Lindeboom, B.M. Mulder, Proceedings of the National Academy of Sciences (2017). DOI 10.1073/pnas.1702650114. URL http://www.pnas.org/content/early/2017/06/15/1702650114.abstract
35. Y. Oda, H. Fukuda, Science **337**(6100), 1333 (2012). DOI 10.1126/science.1222597. URL http://dx.doi.org/10.1126/science.1222597